

# Microhardness and Water Sorption in Injection-Molded Starch

F. ANIA,<sup>1</sup> M. DUNKEL,<sup>2</sup> R. K. BAYER,<sup>2</sup> F. J. BALTÁ-CALLEJA<sup>1</sup>

<sup>1</sup> Instituto de Estructura de la Materia, Consejo Superior de Investigaciones Científicas, Serrano 119, E-28006 Madrid, Spain

<sup>2</sup> Institut für Werkstofftechnik, Universität Kassel, Mönchebergstrasse 3, D-34125 Kassel, Germany

Received 31 July 2001; accepted 25 September 2001

**ABSTRACT:** The microhardness of injection-molded potato starch was investigated in relation to the water sorption mechanism. The creep behavior under the indenter and the temperature dependence of the microhardness are reported. The influence of the drying time on microhardness, weight loss and density changes for materials with different injection-molding temperatures is highlighted. Results reveal the role of the various mechanisms of water evaporation involved. The occurring structural mechanisms are discussed in terms of the gradual transformation of single helices of amylose and amylopectin into a network structure of double helices and the partial destruction of this structure. Experiments on starch samples, heated at 200°C, suggested the occurrence of an extreme densification of the network hindering the water adsorption in a humid atmosphere. © 2002 Wiley Periodicals, Inc. *J Appl Polym Sci* 85: 1246–1252, 2002

**Key words:** polysaccharides; biopolymers; hardness; adsorption

## INTRODUCTION

With the increasing tendency nowadays to use renewable resources, attention has been focused on the possibility of using natural polymers to replace synthetic ones. Starch is a polysaccharide that is produced by photosynthesis in many plants as a form of food storage. Furthermore, starch is a thermoplastic biopolymer that can be transformed by means of conventional thermomechanical treatments with a suitable plasticizer (typically water).<sup>1</sup> The possibility of using starch films in the packaging industry gave rise to early studies on their mechanical properties.<sup>2,3</sup> More recently, the deformation of thin films from extruded starch was investigated.<sup>4</sup> These studies

indicated that extrusion at low temperatures yields nonhomogeneous films showing granule remnants that affect the mechanical performance. The influence of the processing methods on starch properties has been the object of a preceding investigation.<sup>5</sup> Thus, compression molding of starch granules leads to sintered, brittle materials. In the compression-molded samples, the majority of amylopectin crystals remains preserved, as revealed by X-ray diffraction and optical microscopy. The preparation of starch films from gels results in the disintegration of the structure of native starch granules and in the formation of a new structure formed by the crystallization of the linear amylose molecules.<sup>5</sup> On the other hand, injection molding of native starch at temperatures above 80°C has been shown to give rise to amorphous materials with excellent mechanical properties. The elastoplastic properties of injection-molded-starch-based materials

---

Correspondence to: F. J. Baltá-Calleja

*Journal of Applied Polymer Science*, Vol. 85, 1246–1252 (2002)  
© 2002 Wiley Periodicals, Inc.

show a clear hardening on thermal treatment.<sup>6</sup> This hardness increase has been associated with a water decrease detected in these materials. The concept of micromechanical characterization of polymer materials has enjoyed steady growth and popularity in recent years.<sup>7</sup> Particular attention has been given to microhardness ( $H$ ) as a technique capable of detecting morphological and textural changes in polymers.

The purpose of this study was to extend the previous studies and to examine the influence of the water content on  $H$  of injection-molded starch materials exposed to the influence of different thermal treatments and relative humidities.

## EXPERIMENTAL

Native potato starch granules (Emsland Superior Stärke GmbH, Emlichheim, Germany) were used for preparation of the samples. The granules were mixed with 5 wt % water for the injection-molding process. Starch processing is enhanced by the presence of water, which depresses the melting point of the amylopectin crystallites and lowers the starch melt viscosity.<sup>8</sup> With an appropriate temperature, the obtained melt can be injected into a mold at a given pressure. Molded specimens of the usual dumbbell shape for mechanical testing showed a 35-mm central bar with a rectangular cross-section of  $4 \times 5.2$  mm. To perform  $H$  measurements, we cut 2 mm thick sections with a microtome from the center of the samples. Slides ( $45 \mu\text{m}$ ) were also used for water sorption experiments and for the recording of transmission IR spectra. Processing parameters, such as melt temperature ( $T_m$ ) and type of mold (elongational, intermediate, or normal flow), during injection were varied. Preliminary studies showed that a  $10^\circ\text{C}$  step variation of  $T_m$  from  $130$  up to  $180^\circ\text{C}$  did not significantly change the average  $H$  of the samples, which yielded an approximate value of 120 MPa. Hence, only two  $T_m$ 's were chosen for this study: a low temperature of  $100^\circ\text{C}$  and a higher one of  $140^\circ\text{C}$  with nozzle temperatures of  $100$  and  $120^\circ\text{C}$ , respectively. The next step was to determine whether a change of melt flow during the injection process could affect  $H$  values or create any type of anisotropy within the samples. Among all the studied samples, only one, produced under an elongational flow regime, showed a certain increase of the  $H$  values at about 1 mm from both surfaces. However, no hardness difference was found between the flow and the perpen-

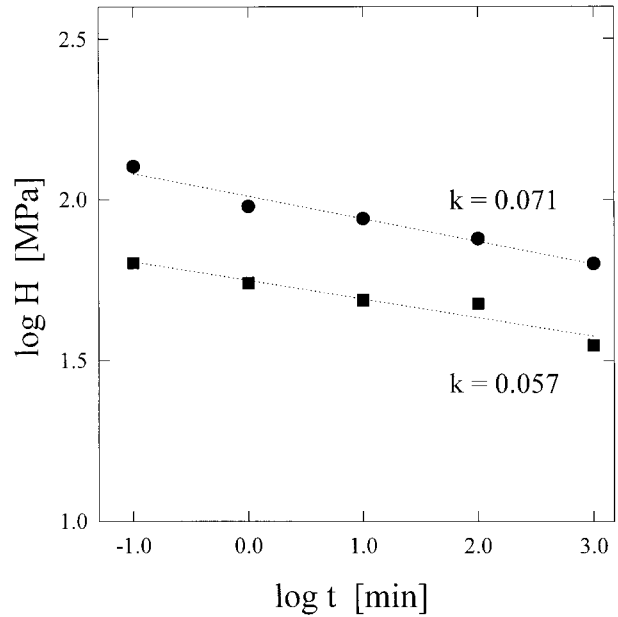


**Figure 1** Log-log plot of  $H$  as a function of loading time for the two materials processed at  $T_m = 100^\circ\text{C}$  (■) and  $T_m = 140^\circ\text{C}$  (●).

dicular directions (no traces of indentation anisotropy). To improve the smoothness of the sample surface and to obtain well-defined indentations, we used diamond paste with a particle size of  $1 \mu\text{m}$  to polish the surfaces. This method temporarily raised the humidity of the sample, producing a decrease in  $H$ . Conventional  $H$  values were recovered after 24 h. Macroscopic density values of 2 mm thick samples were obtained by means of a density gradient column with a mixture of carbon tetrachloride and dioxane. Transmission IR spectra of  $45 \mu\text{m}$  films were recorded with a PerkinElmer Fourier transform infrared (FTIR) spectrometer (PerkinElmer Analytical Instruments, Shelton, CT) with a resolution of  $2 \text{ cm}^{-1}$  after five accumulated scans.

## RESULTS

To compare the mechanical properties of two samples, one processed at low temperature ( $T_m = 100^\circ\text{C}$ ) and the other one injection molded at high temperature ( $140^\circ\text{C}$ ),  $H$  was analyzed as a function of loading time (Fig. 1). The  $H$  values and the hardness rate of decrease with time (creep constant) were lower for the material processed at low  $T_m$ 's, which means that creep was slower for the low-temperature sample. This result suggests

that there must have been some kind of variation in the amorphous structure of both materials to account for the strong differences in mechanical properties observed.

The next step is to determine the temperature dependence of  $H$  for the two previously mentioned materials. We used a constant loading time of 0.1 min, which has been commonly used as a compromise between reproducible hardness measurements and a minimum creep of the material.<sup>7</sup> Measurements were performed at room conditions (i.e., at 25°C and an average relative humidity of 50%). Figure 2 shows that  $H$  values were always higher for the high-temperature material. In addition, at least four temperature intervals could be defined for both injection temperatures where significant  $H$  changes were detected:

1. An  $H$  increase from room temperature up to roughly 40°C.
2. A plateau in the range 40–55°C.
3. A new hardness increase from 55 to 70°C.
4. Finally, when the temperature was greater than 70°C, a clear  $H$  decrease was observed for both samples.

The latter  $H$  decrease could eventually be associated to the presence of the glass transition for

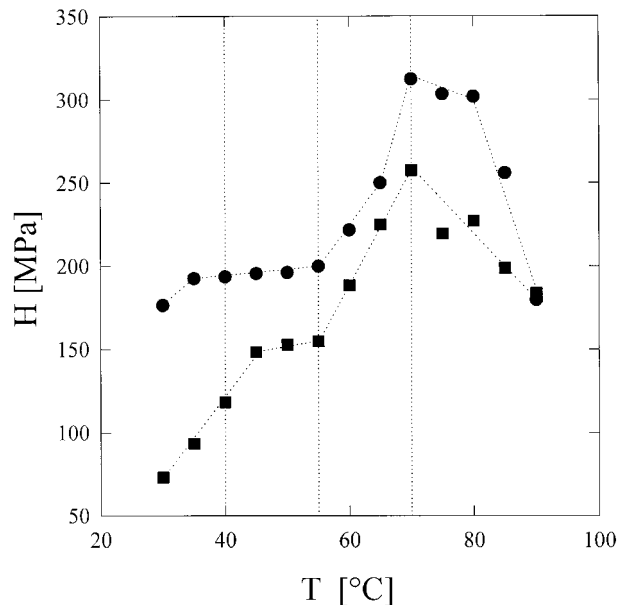


**Figure 2**  $H$  as a function of temperature for the two investigated materials:  $T_m = 100^\circ\text{C}$  (■) and  $T_m = 140^\circ\text{C}$  (●). Vertical lines denote the proposed temperature intervals (see text).

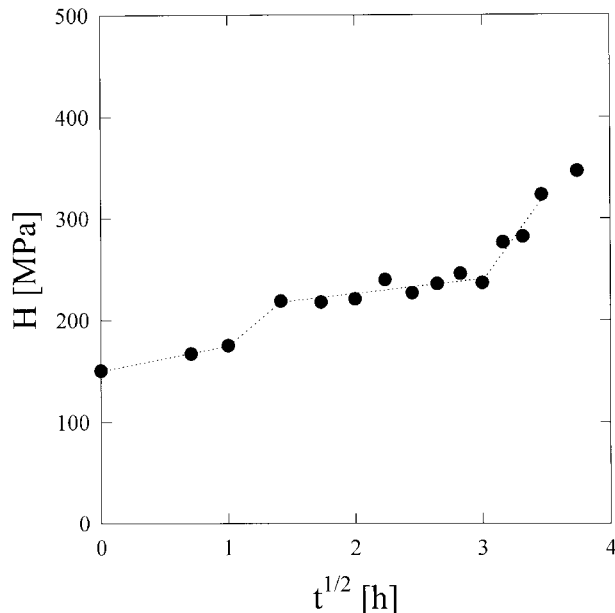


**Figure 3**  $H$  as a function of the square root of drying time at  $70^\circ\text{C}$  for the higher temperature sample ( $T_m = 140^\circ\text{C}$ ).

potato starch. However, it is known<sup>9,10</sup> that the glass transition of partially dried starch occurs at a higher temperature. A possible explanation for the observed results could be related to a modification of the structure that led to a degradation of the mechanical properties.<sup>11</sup>

Figure 3 illustrates for the high-temperature sample ( $T_m = 140^\circ\text{C}$ ) the  $H$  increase as a function of the square root of time  $t$  at  $70^\circ\text{C}$ . This temperature was the highest reachable one that could be used without the occurrence of any structural degradation (Fig. 2). Therefore, we chose to analyze the total water evaporation from the studied injection-molded samples. From this plot, one may attempt to distinguish three different regimes of  $H$  behavior that can be associated with the first three regions in Figure 2.

Another technique, which would also provide information about the water content within starch, is the determination of the macroscopic density. The obtained results are summarized in Figure 4, where density is plotted against the square root of the conditioning time at  $70^\circ\text{C}$ . The final experimental density value of the dry injected sample was  $1520 \pm 5 \text{ kg/m}^3$ . On the other hand, the wet density values were slightly overestimated with increasing water content in the gradient density column because of the existing solubility between water and dioxane. Dioxane

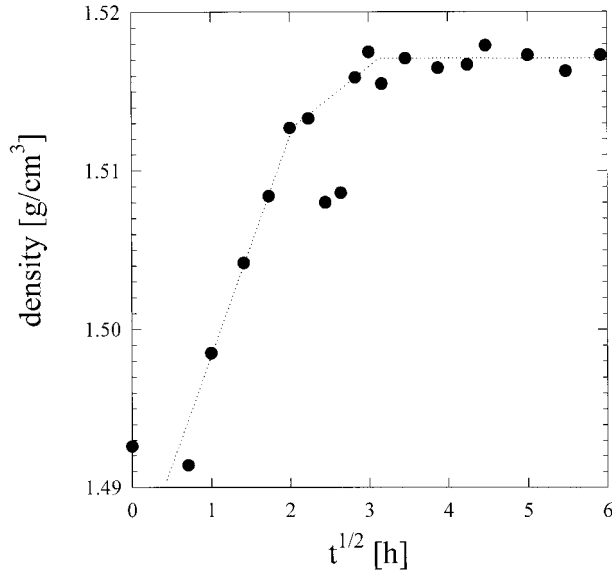


**Figure 4** Density variation as a function of the square root of drying time at 70°C for the higher temperature sample ( $T_m = 140^\circ\text{C}$ ; thickness = 2 mm).

acts as a drying agent in contact with starch because this solvent, although not capable of penetrating into the material due to its large molecular size, produces a certain extraction of water molecules. This effect should explain the large deviation observed for the untreated sample ( $t = 0$ ), which yielded a density value of  $1490 \text{ kg/m}^3$  in contrast to typical values of  $1460 \text{ kg/m}^3$  found in the literature.<sup>12</sup> The change in the slope observed in Figure 4 in the 6–8 h time interval could again be related to the previously mentioned time intervals in Figures 2 and 3.

## DISCUSSION

### Hardness Variation on Water Removal: Temperature and Time Dependence

The different regimes, observed as a function of temperature in Figures 2 and 3, could be addressed in terms of the different degrees of bound water present in the samples, a concept that has been often used to account for the different NMR relaxation times of water molecules found with increasing amount of adsorbed water in starch.<sup>13</sup> However, according to calculations performed on an atomistic model for amorphous starch with different water contents,<sup>8</sup> the binding energy of water is constant with increasing water content. This means that each water molecule tends to

form four hydrogen bonds, irrespective of whether the surrounding partner is starch or other water molecules, a result that seems to rule out the existence of specially bound water. However, as excess energy of evaporation is actually observed to increase with decreasing water content, this excess was attributed to changes in the starch matrix on addition or removal of water molecules.<sup>8</sup> In preceding studies,<sup>14,15</sup> the analysis of the X-ray diffraction patterns of processed starch offered a possible explanation about the structural changes occurring on injection-molded materials as a function of temperature. Accordingly, the first interval ( $H$  increase) can be associated to a transformation of the majority of single helices into a network structure of double helices. The plateau, showing a constant  $H$ , could be due to the combination of two opposing effects: a densification of hard elements, which are the double helices, and the partial destruction of some of these elements. Finally, the second  $H$  increase found between 55 and 70°C could be associated with the end of the plasticizing effect of water and the increasing amount of contacts among starch molecules.

### Weight Loss Analysis: Influence of Sample Thickness

Considering that the  $H$  increase, observed in Figures 2 and 3, was mainly related to the water evaporation from the sample, we discuss next the weight decrease as a function of time, which was achieved by conditioning the material at 70°C. It was evident that the thickness of the sample played here an important role in the water content evolution. Figure 5(a,b) illustrates the weight loss evolution for two samples 45  $\mu\text{m}$  and 2 mm thick, respectively. As expected, the thinner sample (prepared at both processing temperatures) lost a large amount of water in the first 2 min [Fig. 5(a)]. The whole drying process was completed a few minutes later. On the contrary, the 2 mm thick sample showed a rather continuous weight loss behavior, which made it difficult to distinguish between the different mechanisms due to their mutual superposition [Fig. 5(b)].

Table I summarizes the different adsorption/desorption limits of the thicker and thinner samples for the two investigated materials. A set of samples stored for 24 h at room conditions were weighted. Thereafter, half of the samples were dried at 70°C, and the other half were stored again in a humid atmosphere until weight con-

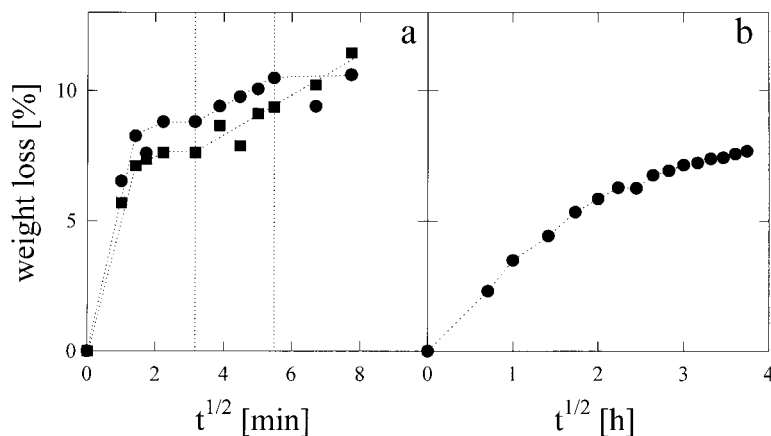


**Figure 5** Weight loss as a function of the square root of drying time at 70°C for two different sample thickness: (a) 45  $\mu\text{m}$  and (b) 2 mm.

stancy was reached. The differences between the initial weight values at room conditions and the final, dry or humid, values are collected in Table I. According to these data, although the 2 mm thick samples seemed to contain a higher proportion of water than the thinner counterparts under normal conditions, this was a clear artifact due to the instant uptake of water of the dry samples during the weight measurement. Both type of samples should have contained similar relative amounts of water provided the same initial state of equilibrium. On the other hand, after the measured time thick samples showed a lower relative capture of water in a humid atmosphere. The total weight difference (from dry to humid) was always lower for the thick samples, due to the more difficult access to the inner regions. From the viewpoint of processing, it is noteworthy that the structure developed by the sample injected at high temperature seemed to be able to accommodate a smaller

amount of water than the low-temperature one (last line in Table I).

Most interesting is the plot of the  $H$  increase (Fig. 3) as a function of the weight decrease measured, shown in Figure 5(b). Figure 6 reveals that the strongest increase (2/3) of  $H$  did not correspond to the initial 7% weight loss but rather to the final 3%. In accordance with Figure 2, this would mean that the more pronounced  $H$  enhancement corresponded to the interval where the last traces of water were evaporating and could not act any more as a material softener.

**Table I** Relative Weight Variation (%) as Compared with Ambient Conditions of Two Samples, Both Dry and Humid, with Different Thicknesses

	$T_m$			
	140°C		100°C	
	45 $\mu\text{m}$	2 mm	45 $\mu\text{m}$	2 mm
Dry	-6.2	-7.6	-9.2	-12.2
Humid	11.5	5.9	11.1	3.9
Difference	17.7	13.5	20.3	16.1

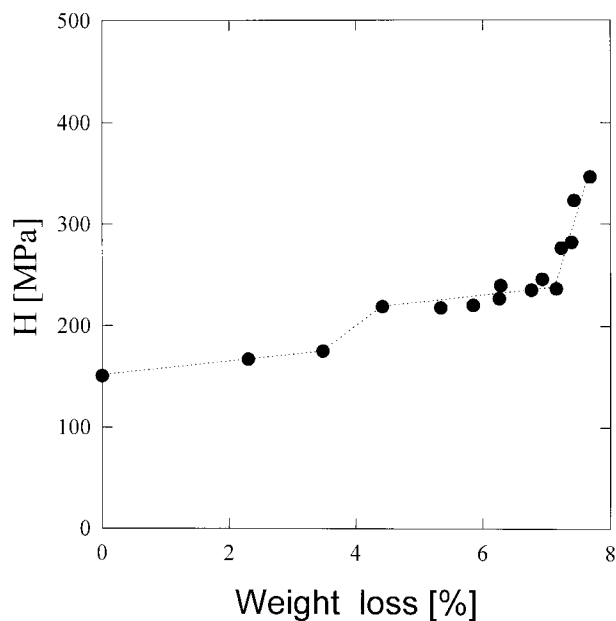


**Figure 6**  $H$  data of Figure 3 plotted as a function of the weight loss of Figure 5(b).

This notorious  $H$  increase probably could be associated to the third mechanism of evaporation, as proposed in ref. 15.

### High-Temperature Treatment

In view of the higher  $H$  values obtained for the higher injection-molding temperature ( $T_m = 140^\circ\text{C}$ ; see Fig. 2), we tested a simple method of structure modification at a still higher temperature ( $200^\circ\text{C}$ ) for a very short time to prevent degradation. We aimed here to attempt to stabilize the  $H$  increase of starch by hindering the water penetration. We studied the detailed weight loss of water due to treatment at  $200^\circ\text{C}$  by FTIR spectroscopy by following the band corresponding to the O—H deformation modes at  $1640\text{ cm}^{-1}$  (Fig. 7).<sup>16</sup> A Fickian diffusion, typical for high-temperature treatments,<sup>15</sup> was observed. Practically all the water was lost after the first 30 s of thermal treatment without any appreciable changes in the other IR bands. Figure 8 shows the different behavior of the two injection-molded samples ( $T_m$ 's = 100 and  $140^\circ\text{C}$ ) heated at  $200^\circ\text{C}$  for various times with reference to the adsorption of water in a humid atmosphere. Figure 8 also illustrates the excess of the water increase in relation to a reference sample that was kept in a normal atmo-

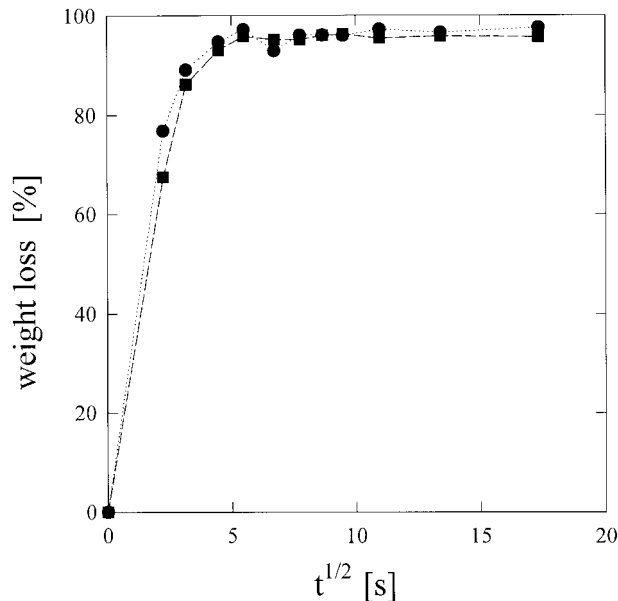


**Figure 7** Weight loss in real time as a function of the square root of treatment time at  $200^\circ\text{C}$  followed by FTIR for  $45\text{ }\mu\text{m}$  samples:  $T_m = 100^\circ\text{C}$  (■) and  $T_m = 140^\circ\text{C}$  (●).

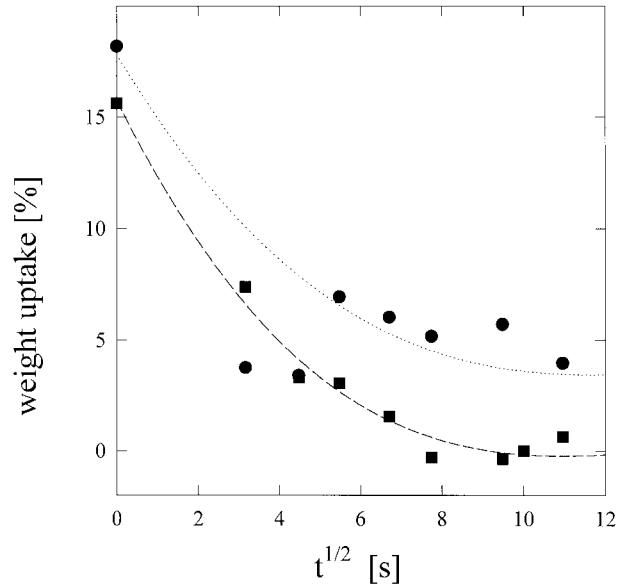


**Figure 8** Relative water weight uptake for the two injection-molded materials treated at  $200^\circ\text{C}$  for different times and thereafter exposed to a humid atmosphere for 24 h:  $T_m = 100^\circ\text{C}$  (■) and  $T_m = 140^\circ\text{C}$  (●).

sphere. For  $t = 0$ , samples adsorbed more than 15% excess water than they did in the initial state. The adsorption capacity was hindered with increasing treatment time at  $200^\circ\text{C}$ . The samples that were dried at  $200^\circ\text{C}$ , despite the drastic decrease in water content, showed a considerable resistance against water adsorption in a humid atmosphere. In the extreme case of a fully dried sample (100 s at  $200^\circ\text{C}$ ), no more water was adsorbed in a humid atmosphere (see Fig. 7). This finding could be discussed as an extreme densification of the network of double helices that hindered the penetration of water molecules within the material.

### CONCLUSIONS

1. The dependence of  $H$  on the annealing temperature of injection-molded starch can be discussed in terms of three different temperature intervals corresponding to characteristic structural changes.
2. These three regimes can be also characterized in an isothermal experiment as a function of diffusion time.
3. The first regime involves a  $H$  increase correlated to a strong weight loss of water. The second regime corresponds to a con-

stancy of the  $H$  value that is associated with a lower evaporation rate. The third regime is revealed by a very sharp  $H$  increase that is associated with the evaporation of the small amount of remaining water.

4. The first mechanism is associated with the structural transformation of the majority of single helices into double helices of amylopectin. This is followed by a second mechanism, where the densification of hard elements (double helices) and a partial destruction of some of these elements take place simultaneously. Finally, the third mechanism might be correlated to the end of the plasticizing effect of water and the increasing amount of intermolecular contacts among starch molecules.
5. The temperature of injection modifies the amorphous structure of injection-molded starch, which results in a higher  $H$  for the higher injection temperature ( $T_m = 140^\circ\text{C}$ ). Starch samples annealed for short times at still higher temperatures ( $200^\circ\text{C}$ ) exhibit an enhanced resistance to water penetration.

## REFERENCES

1. Poutanen, J.; Forssell, P. *Trends Polym Sci* 1996, 4, 128.
2. Mark, A. M.; Roth, C. L.; Mehlretter, I. L.; Rist, C. E. *Cereal Chem* 1964, 41, 197.
3. Nakamura, S.; Tobolsky, A. V. *J Appl Polym Sci* 1967, 11, 1371.
4. Warburton, S. C.; Donald, A. M.; Smith, A. C. *Carbohydr Polym* 1993, 21, 17.
5. Baltá Calleja, F. J.; Rueda, D. R.; Secall, T.; Bayer, R. K.; Schlimmer, M. *J Macromol Sci Phys B* 1999, 38, 461.
6. Flores, A.; Bayer, R. K.; Krawietz, K.; Baltá Calleja, F. J. *J Macromol Sci Phys B* 2000, 39, 751.
7. Baltá Calleja, F. J.; Fakirov, S. *Microhardness of Polymers*; Cambridge University Press: Cambridge, England, 2000.
8. Trommsdorff, U.; Tomka, I. *Macromolecules* 1995, 28, 6138.
9. Benczédi, D.; Tomka, I.; Escher, F. *Macromolecules* 1998, 31, 3055.
10. Zeleznak, K. J.; Hosenev, R. J. *Cereal Chem* 1987, 64, 121.
11. Willenbücher, R. W. Ph.D. Thesis 10136, Eidgenössische Technische Hochschule Zurich, 1993.
12. van Soest, J. J. G.; Essers, P. *J Macromol Sci Pure Appl Chem A* 1997, 34, 1665.
13. Lechert, H. *Stärke* 1976, 28, 369.
14. Shefer, A.; Shefer, S.; Kost, J.; Langer, R. *Macromolecules* 1992, 25, 6756.
15. Bayer, R. K.; Lindemann, S.; Dunkel, M.; Cagliaio, M. E.; Ania, F. *J Macromol Sci Phys B* 2001, 40, 733.
16. Rao, C. N. R. *Chemical Applications of Infrared Spectroscopy*; Academic: New York, 1963.